IOPscience iopscience.iop.org

Home Search Collections Journals About Contact us My IOPscience

Deep disorder in neon-implanted copper single crystals detected by variable-energy positrons

This article has been downloaded from IOPscience. Please scroll down to see the full text article.

1989 J. Phys.: Condens. Matter 1 5411

(http://iopscience.iop.org/0953-8984/1/32/010)

View the table of contents for this issue, or go to the journal homepage for more

Download details:
IP Address: 171.66.16.93
The article was downloaded on 10/05/2010 at 18:36

Please note that terms and conditions apply.

J. Phys.: Condens. Matter 1 (1989) 5411–5419. Printed in the UK

Deep disorder in neon-implanted copper single crystals detected by variable-energy positrons

R S Brusa†, A Dupasquier‡, R Grisenti†, S Liu†§, S Oss† and A Zecca†
† Dipartimento di Fisica, Università di Trento, 38050 Povo TN, Italy
‡ Istituto di Fisica del Politecnico, Piazza L. da Vinci, 32,20133 Milano MI, Italy

Received 24 November 1988, in final form 27 January 1989

Abstract. A positron beam with variable energy up to 30 keV has been used to observe defects created by Ne ion implantation in Cu single crystals. The density profile of these defects has a peak centred at a depth much larger than the ion implantation depth; this result is interpreted as being due to dislocation loops formed by aggregation of self-interstitials.

1. Introduction

Lattice disorders produced by ion implantation in metals have been the subject of a number of transmission electron microscopy (TEM) studies (for reviews, see [1–3]), which have given detailed information on the amount, species and localisation of defects in various materials under different conditions. The thorough exploration made in the past years leaves little room for new TEM studies; however, it may be interesting to return to this subject with an entirely different experimental approach that can demonstrate effects not easily detected by TEM. This is the case with the recently developed positron beam technique, which is used in the present work to detect defects created in Cu single crystals by Ne ion implantation. Special attention is paid to regions deeper than the ion implantation profile. Deep lattice disorders in an ion-implanted crystal may come from self-interstitials forming mobile dislocation loops ('interstitial' loops), which migrate in the material until they can escape from a free surface or stop at an obstacle. Interstitial loops are however not usually observed by TEM in single crystals of pure FCC metals (for examples and discussions, see [4–6]) because of the escape of mobile loops from the free surfaces of the thin samples used for TEM studies. This problem does not exist for the positron beam technique, which allows deep exploration of semi-infinite samples.

The use of positrons for depth-resolved analyses of defects in the proximity of a surface is a recent extension of well known methods of defect detection, based on the phenomenon of positron trapping at lattice sites where one or more ions are missing, or where the structure is less densely packed than in the regular lattice (extended reviews of positron annihilation in solids and applications to solid state studies can be found in [7, 8]). In traditional applications, the positrons are implanted in the sample at the energy they have when emitted from a radioactive source; the depth of the explored region is therefore fixed by the choice of the emitting isotope. In recent years, however,

§ Permanent address: Institute for Metal Research, Academia Sinica, Wenhua Road, Shenyang, People's Republic of China.

0953-8984/89/325411 + 09 $02.50 © 1989 IOP Publishing Ltd

the development of variable-energy positron beams has given more flexibility to the method, since by controlling the positron implantation energy one can probe a sample at different depths.

Information on the presence and localisation of defects can be obtained using two different experimental approaches: (1) to observe the dependence of annihilation characteristics on the positron implantation energy [9, 10], and (2) to measure the current of positrons diffusing back to the surface after thermalisation in the sample [11]. The two techniques can be used in combination, but in fact a choice is dictated by the extension of the region to be explored: when defects are localised at depths above the diffusion length of the positrons in the sample, which is of the order of 100 nm for most metals in the absence of defects, the positron current returning to the surface from the defect region can be too small to yield satisfactory accuracy. For this reason, in the present study of defect profiles extended well beyond the positron diffusion length, we adopt the first of the above alternatives in the same version used in [9, 10], i.e., by measuring variations in the Doppler broadening of the annihilation line at 511 keV. Details of our experimental procedure are given in § 2.

With the Doppler broadening technique, the signature of lattice defects encountered by the positrons is the narrowing of the annihilation line [12], corresponding to the narrowing of the electron momentum distribution probed by a positron trapped in an open-volume defect, as compared to the momentum distribution probed in the bulk of the material. In the presence of a non-uniform defect distribution, the dependence of the line width on the beam energy displays structures not existent for a homogeneous reference sample. From the position and the shape of these structures, one can obtain quantitative information on the spatial localisation and on the shape of the defect density profile. However, the analysis of the raw experimental data is not immediate: information on the defect distribution is obtained in a convoluted form with the spatial distribution of the annihilation sites, determined not only by the positron implant profile but also by the defect distribution itself. This requires a more or less sophisticated mathematical model; our approach will be discussed below, but in any case, the prerequisites for a reliable analysis are: a distribution of annihilation sites not too broad in comparison with the structures of the defect profile, and a large specific effect on the line width of positron trapping in defects.

The first condition sets an upper limit to the depths that can be explored, because the width of the positron implantation profile increases with the mean depth [13]; the practical limit is of the order of 1 μm. The fulfilment of the second condition depends critically on the nature of the lattice defect acting as a positron trap; the rule is that the specific variation in the line width increases with the size of the defect, with saturation for large sizes. The experiments reported in [9–11] have shown that the effect on the line width of helium bubbles, formed by diffusion of helium ions implanted at fluences from 4×10^{16} to 2.5×10^{17} ions/cm^2, is fully adequate for the applicability of the method; quite recently, indications of good sensitivity at much lower fluences (10^{13} He ions/cm^2) have also been presented [14]. Here we have an intermediate fluence (10^{15} Ne ions/cm^2), but we expect a weaker signal from dislocation loops than from gas-filled bubbles. Nevertheless, the results presented in § 2 leave no doubt as to the applicability of the method even in this situation. The quantitative analysis of our data is based on a numerical procedure that provides complete flexibility concerning assumptions on defect and positron implant profiles; this is described in § 3. The results of the analysis are discussed in § 4.

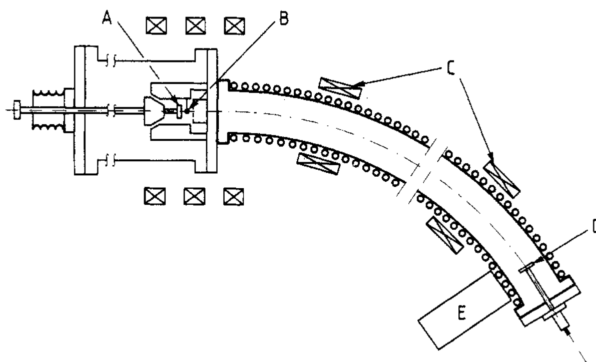

Figure 1. Schematic view of the apparatus. (A) W(100) moderator; (B) ^{58}Co source; (C) correction coils; (D) sample; (E) Ge detector.

2. Experimental procedure and results

Our samples were (100)-oriented Cu single crystals in form of discs (12 mm diameter × 1 mm thick), supplied by Crystaltech, Grenoble. Prior to ion implantation, the samples were etched in sulphamic acid and annealed at 1050 °C for 2 h; cooling rates were 10 °C min^{-1} from 1050 °C to 800 °C, and 8 °C min^{-1} from 800 °C to 20 °C. Three samples were implanted with a fluence of 10^{15} Ne ions/cm^2 at energies of 30, 65 and 100 keV; the ion current densities were 0.5 μA cm^{-2} for the 30 keV sample, 1 μA cm^{-2} for the remaining samples; the sample temperature during implantation was about 100 °C. A non-implanted sample was kept for reference.

The positron beam was obtained by moderating the β^+ spectrum emitted by a 30 mCi ^{58}Co source and then by re-accelerating slow positrons to a final energy, variable between 0.2 and 30 keV. The well known physical principles of beam production by moderation have been presented in various review papers [15–17]; therefore here we give only a few details on the characteristics of our apparatus, which is shown schematically in figure 1. The moderator is a (100)-oriented W single crystal, initially annealed above 2200 °C at a pressure of 6×10^{-9} Torr; the moderation efficiency obtained in the backscattering geometry varied during the experiment (after several exposures to the atmosphere and permanent operation at 10^{-7} Torr) from 1×10^{-3} to 7×10^{-4}. Slow positrons reemitted from the W moderator are injected into the transport system at an energy of 200 eV by an electrostatic extraction stage with a grid aperture. The transport system and energy filter is a 45° bent solenoid 35 mm in diameter, with an axial field of 50 G and a non-axial field in the region of the bend given by two external coils, used for correcting the alignment of the beam with the solenoid axis. The final acceleration was achieved by polarising the target at the desired negative voltage; we avoided magnetic field gradients in the proximity of the target by inserting the target for 15 cm inside the solenoid. The negative polarisation ensured that any positron re-emitted inelastically from the sample returned on the sample itself. By temporarily substituting the sample with a channeltron, and using a series of apertures on the solenoid axis, we ascertained that more than 95% of the beam current hit a central spot 6 mm in diameter when the correction coils were properly adjusted and the acceleration voltage was set at a minimum of 1000 V.

The annihilation radiation emerging from the target through the solenoid wall was detected using an intrinsic Ge detector (efficiency 11%, resolution 1.5 keV for the ^{107}Ru

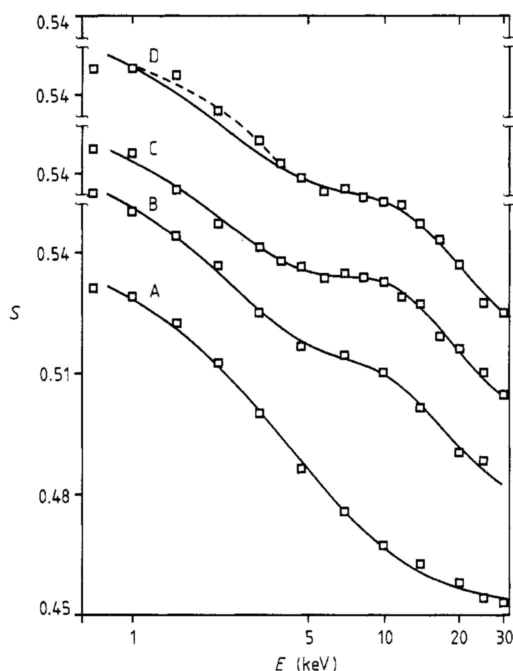

Figure 2. Doppler-broadening lineshape parameter S against incident positron beam energy E. The curves are calculated according to the diffusion model described in the text; a fit including two capture profiles is shown only for the sample implanted at 100 keV (broken curve). A, Annealed Cu; B, Ne-implanted Cu (30 keV); C, Ne-implanted Cu (65 keV); D, Ne-implanted Cu (100 keV).

line at 497 keV). Spectrometer drifts were detected, and were automatically corrected via software by taking the 511 keV annihilation line and the 384 keV line of ^{133}Ba as fixed points. The line width was characterised by means of the usual line shape parameter S, defined as the fractional area of a central section of the annihilation line. In the present work, a width of 0.8 keV was chosen for this section. Partial data were taken at each setting of the beam energy for 5 min, and summed over automatically repeated runs until a total of about 10^6 counts were accumulated at each energy.

Our experimental results for the parameter S are reported in figure 2; the lines through the experimental points are best-fit curves obtained as discussed in § 3. The points below 1 keV, which probably reflect incomplete collection of the beam at low energy, were not included in the fitting procedure.

3. Data analysis

The aim of the analytical procedure was to reconstruct the defect density profile starting from experimental S–E data. For this, we need to give an explicit form to the relationship between S and the defect profile, which comes from the influence that defects localised at different depths have on positrons diffusing in the sample. We follow here the same approach described in [10], but with technical differences in the mathematical treatment to give an unrestricted choice for the class of functions taken for approximating the positron implantation distribution and the defect density profile.

The starting point is to assume that each annihilation event comes from a positron originally in one of the following states: (*a*) a free diffusing state, populated by a fraction f_f of the positron ensemble, and giving annihilations with a characteristic line shape parameter S_f; (*b*) a surface-trapped state (population fraction f_s, line shape parameter

S_s); (*c*) one or more bound states, localised at defects of one or more different families distributed with density $C_i(x)$ at the depth x below the surface (population fraction $f_{d,i}$, line shape parameter $S_{d,i}$ for state i). The experimental annihilation line comes from the statistical superposition of events from the different annihilation channels, leading to an S-parameter that is a linear combination of the specific S-parameters for each channel, as given by:

$$S = S_f f_f + S_s f_s + \sum_i S_{d,i} f_{d,i}. \tag{1}$$

If $n(x)$ is the stationary free positron density at a distance x from the surface (a one-dimensional geometry is appropriate for the present situation), τ^{-1} the annihilation rate of free positrons, D_+ the free positron diffusion constant, and μ_i the specific defect trapping rate, the expressions of the fractions f are:

$$f_f = \tau^{-1} \int_0^\infty n(x)\, dx \tag{2}$$

$$f_s = D_+ (dn/dx)_{x=0} \tag{3}$$

$$f_{d,i} = \mu_i \int_0^\infty C_i(x) n(x)\, dx. \tag{4}$$

In the above equations, the condition

$$f_f + f_s + \sum_i f_i = 1 \tag{5}$$

follows from the proper normalisation of $n(x)$. Equation 3 comes from the assumption of a 'black' surface, i.e., that the diffusion current is totally absorbed in the surface state; we return on this point below.

If non-thermal annihilation and capture are neglected, the stationary distribution $n(x)$ is the solution of the diffusion equation that expresses the balance between incoming positrons, implanted with a profile $P(x)$, and positrons removed from the distribution $n(x)$ by annihilation, trapping or diffusion to the absorbing surface:

$$D_+ (d^2n/dx^2) - \left(\tau^{-1} + \sum_i \mu_i C_i(x)\right) n + P(x) = 0 \tag{6}$$

with the boundary conditions:

$$n(x = 0) = n(x = \infty) = 0. \tag{7}$$

The correct normalisation for $n(x)$ is automatically ensured if one takes:

$$\int_0^\infty P(x)\, dx = 1. \tag{8}$$

Equations (1)–(8) enable one to evaluate S as a functional of $C_i(x)$ and $P(x)$ by passing through the integration of equation (6), which we perform by the numerical routine described in [18]. Functions $C_i(x)$ are however not known *a priori*; thus one has to guess a suitable functional form with parameters to be determined by best fitting with the experimental data. We proceed as follows:

(*a*) for $P(x)$ we take the Valkealathi–Nieminen [11] formula:

$$P(x) = -\mathrm{d}\{\exp[-(x/x_0)^{1.9}]\}/\mathrm{d}x \tag{9}$$

where x_0 is related to the mean implantation depth X:

$$x_0 = X/1.13. \tag{10}$$

In turn, X depends on the beam energy E:

$$X = (D_+\tau)^{1/2}(E/E_0)^n \tag{11}$$

where E_0 and n are parameters determined, together with S_f and S_s, by best fitting to the experimental S-data for the unimplanted reference sample. Based on values for D_+ and τ reported in [15], one has $(D_+\tau)^{1/2} = 109$ nm;

(*b*) First we attempt to fit the experimental data for the implanted sample by assuming the existence of a single defect species; for the product $\tau\mu C(x)$, hereafter called the 'capture profile' and denoted $k(x)$, we assume the form:

$$k(x) = -K\,\mathrm{d}\{\exp[-(x/x_\mathrm{d})^m]\}/\mathrm{d}x \tag{12}$$

where the parameters K, x_d and m are determined, together with S_s and S_d, by best fitting to the experimental S-data for the implanted samples. Here we can state explicitly that in the best fit for the implanted samples we use the values of S_f, E_0 and n obtained from the reference sample data, and we again leave S_s as an adjustable parameter. The reason is that the surface conditions of different samples are not necessarily identical, and small variations in S_s are to be expected; it would be incorrect to cancel these variations with an artificial offset to the data, as this would displace the horizontal asymptote of S for $x = \infty$.

The results of the best-fitting procedure based on this model are shown as full curves in figure 2. For the reference sample and for samples implanted at 30 and 65 keV the variances of the fit (χ^2 per degree of freedom) are 1.5, 1.6 and 1.2, respectively; for the sample implanted at 100 keV, the variance is 2, and an inspection of the figure tells us that the higher discrepancy essentially comes from the low positron energy region. We therefore attempted to improve the fit at 100 keV by assuming the presence of two distinct families of positron traps localised at different depths. However, because the introduction of a second capture profile leads to much heavier best-fit calculations, we made only a partial adjustment by keeping fixed the parameters of the capture profile obtained in the preliminary three-state fit; for the additional defect family, we again took the shape given by equation (12) with K, x_d and m as free parameters. The result is the broken curve in figure 2, which merges with the solid curve at high positron energy; the variance of this fit is 1.1.

4. Results of the analysis and comments

Our best-fit values for the free parameters in equation (10) are $E_0 = 4.35$ keV and $n = 1.13$; we have here a discrepancy with [13, 19], which for Cu give n from 1.4 to 1.6, as well as a penetration depth at 1 keV from which one obtains $E_0 \simeq 8$ keV. A modification of our mathematical model to include an internal reflection coefficient at the surface would bring our values in better agreement with the literature, at the cost of increasing the number of parameters to be adjusted. However, we avoid forcing the analysis in this

Table 1. Mean depths of the capture profiles (x_d) and of the ion implantation profiles (R).

Ion energy (keV)	x_d (nm)	R^a (nm)
30	381	25
65	410	46
100	65 and 417	71

[a] Calculated according to Dearnley *et al* [22].

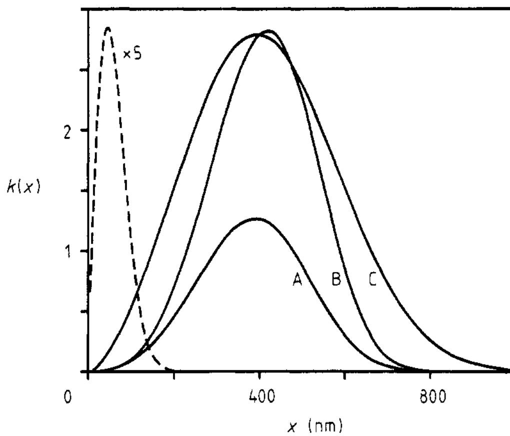

Figure 3. Best-fit evaluation of the capture profiles $k(x)$; the contribution of shallow defects is shown only for the sample implanted at 100 keV (broken curve). Ne-implanted Cu sample at A, 30 keV; B, 65 keV; C, 100 keV.

direction because the shape and the depth of the positron implantation distribution may actually depend on the specific experimental arrangement.

An important parameter is the voltage difference between the sample and the chamber walls; with the negative bias used in the experiment, the positrons escaping from the sample after incomplete thermalisation are re-implanted near the surface. We recall that effects due to epithermal positrons have been observed in Cu at implantation energies up to 6 keV [20]. Also positron channelling [21] may be important, since the incidence of the re-accelerated beam is almost normal to the (100) surface of the sample.

The mean depth values for the capture profiles as obtained from the best-fitting analysis are given in table 1; the functions $k(x)$ representing the shape of the profiles are shown in figure 3. The area below each curve (not including the dashed peak for the 100 keV sample), i.e., the parameter K in equation (12), has been constrained to be proportional to the total energy released during ion implantation. The fit is not very sensitive to K; variations within 20% are compensated by correlated small variations in S_d. Even less precise is the determination of the height of the left peak for the 100 keV sample, which is based on data in a very restricted energy interval; realistically, one can take the height reported in figure 3 as an indication of the order of magnitude. On the contrary, from the statistical point of view, the determination of the depth is much more precise: we estimate the statistical error of the mean depths reported in table 1 at about 2.5%. However, the depth scale depends non-linearly on the parameters E_0 and n

introduced as fixed values in the analysis for the implanted samples. For instance, a scale based on the values given in [13] gives 100 nm, 300 nm and 1000 nm, where we have 200 nm, 400 nm and 1000 nm, respectively. For this reason, we cannot exclude systematic error much larger than purely statistical uncertainty.

The above discussion on the overall accuracy obtained in this experiment does not affect the main information given by our results: the structure in the S–E curve observed at high beam energy demonstrates positron trapping in the region of disorder much deeper than the mean ion implantation depth (also reported in table 1 for comparison). By combining the present evidence with the results of TEM studies, we conclude that this region is the interstitial counterpart of the vacancy-type disorder observed by TEM within the ion implantation range. The attribution is consistent with the observation that the position of the peak is not correlated to the ion implantation energy: the repulsion of self-interstitials from the implanted region is due to the compression generated for accommodating the large local concentration of implanted ions, which is proportional to the fluence and not to the energy. We also remark that our interpretation is not in contrast with the well known fact that interstitials do not trap positrons, but it implies partial reordering leading to the formation of interstitial loops: in this case the capture of positrons occurs in the expanded zone at the edges of portions of regular lattice planes.

The narrow peak in the capture profile for the sample implanted at 100 keV is most probably due to gas-filled bubbles and dislocation loops formed by the collapse of vacancy aggregates within the implantation region. Traces of a similar peak also seem to exist in our data for samples implanted at lower energies, but the data quality does not allow us to attempt a reconstruction. Not only does the lower implantation energy produce a smaller concentration of defects, but also the position of the peak moves in a region closer to the surface that we cannot explore in detail due to the limitations of our set-up below 1 keV. In the absence of data at very low positron energy, the fitting procedure masks the effect of capture in the proximity of the surface by adjusting the apparent surface value of the S-parameter.

The second aspect of our results is a contribution to the elucidation of the potential of the positron beam technique. In summary, our work demonstrates: (*a*) the possibility of using a variable-energy positron beam for material studies in conditions that are unfavourable for TEM analyses; (*b*) the sensitivity of the method not only to bubbles and voids but also to dislocations; (*c*) the flexibility of the numerical analysis of the data in a case with a complicated defect distribution. On the other hand, a negative point is that, in the absence of a fixed reference point the depth scale must be determined in an indirect way, and may be affected by our imperfect knowledge of the positron implantation distribution as well as by arbitrary choice in the mathematical model.

Acknowledgments

We thank Della Mea who implanted the samples used in these measurements. We are indebted to A Seeger and G Kogel for illuminating discussions on mobile defects in irradiated crystals, and to L Quartapelle for his help in the numerical analysis of the data. Positron research at the University of Trento and at the Politecnico di Milano is jointly supported by the Consiglio Nazionale delle Ricerche and the Ministero della Pubblica Istruzione. S Liu benefited from the personal support of the International Centre for Theoretical Physics, Trieste, Italy. The Trento group was partially supported by the Istituto per la Ricerca Scientifica e Tecnologica, Trento.

References

[1] Eyre B L 1973 *J. Phys. F: Met. Phys.* **3** 422
[2] Wilkens M 1975 *Fundamental Aspects of Radiation Damage in Metals* ed. M T Robinson and F W Young Jr USERDA Conf. 751006-PI p 98
[3] Jäger W 1981 *J. Microsc. Spectrosc. Electron* **6** 437
[4] Häussermann F 1972 *Phil. Mag.* **25** 537
[5] Stathopoulos A Y 1981 *Phil. Mag.* A **44** 285
[6] Jager W and Merkle K L 1988 *Phil. Mag.* A **57** 479
[7] Hautojärvi P (ed.) 1979 *Topics in Current Physics* **12** (Berlin: Springer)
[8] Brandt W and Dupasquier A (eds) 1983 *Positron Solid State Physics* (Amsterdam: North-Holland)
[9] Triftshäuser W and Kögel G 1983 *Phys. Rev. Lett.* **48** 1741
Kögel G and Triftshäuser W 1983 *Radiat. Eff.* **78** 221
[10] Lynn K G, Chen D M, Nielsen B, Pareja R and Myers S 1986 *Phys. Rev.* B **34** 1449
[11] Vehanen A, Makinen J, Hautojärvi P, Huomo H and Lahtinen J 1985 *Phys. Rev.* B **32** 7561
Makinen J, Vehanen A, Hautojärvi P, Huomo H, Lahtinen J, Nieminen R M and Valkealahti S 1986 *Surf. Sci.* **175** 385
[12] MacKenzie I K, Eady J A and Gingerich R R 1970 *Phys. Lett.* **33A** 279
[13] Valkealathi S and Nieminen R M 1983 *Appl. Phys.* A **32** 95
[14] Uedono A, Tanigawa S and Sakairi H 1988 *Positron Annihilation* ed. L Dorikens-Vanpraet, M Dorikens and D Segers (Singapore: World Scientific) p 413
[15] Mills A P Jr see ref. [8] p 432
[16] Dupasquier A and Zecca A 1985 *Riv. Nuovo Cimento* **8** 12
[17] Lynn K G and Schultz P J 1988 *Rev. Mod. Phys.* **60** 701
[18] Dupasquier A and Quartapelle L 1987 *Appl. Phys.* A **44** 239
[19] Mills A P Jr and Wilson R 1982 *Phys. Rev.* A **26** 490
[20] Huomo H, Vehanen A, Bentzon M D and Hautojärvi P 1987 *Phys. Rev.* B **35** 8252
[21] Schultz P J, Logan R, Jackman T E and Davies J A 1989 *Phys. Rev.* B **38** 6369
[22] Dearnley G, Freeman J H, Nelson R S and Stephen J 1973 *Ion Implantation* (Amsterdam: North-Holland) p 766